



CHORUS

This is the accepted manuscript made available via CHORUS. The article has been published as:

Inhibiting Klein Tunneling in a Graphene p-n Junction without an External Magnetic Field

Hyungju Oh, Sinisa Coh, Young-Woo Son, and Marvin L. Cohen

Phys. Rev. Lett. **117**, 016804 — Published 30 June 2016

DOI: [10.1103/PhysRevLett.117.016804](https://doi.org/10.1103/PhysRevLett.117.016804)

Inhibiting Klein tunneling in graphene p–n junction without an external magnetic field

Hyungju Oh,^{1,2,*} Sinisa Coh,^{1,2} Young-Woo Son,^{1,2,3} and Marvin L. Cohen^{1,2}

¹*Department of Physics, University of California, Berkeley, California 94720, USA*

²*Materials Sciences Division, Lawrence Berkeley National Laboratory, Berkeley, California 94720, USA*

³*Korea Institute for Advanced Study, Hoegiro 85, Seoul 02455, Korea.*

(Dated: May 19, 2016)

We study by first-principles calculations a densely packed island of organic molecules (F_4TCNQ) adsorbed on graphene. We find that with electron doping the island naturally forms a p–n junction in the graphene sheet. For example, a doping level of $\sim 3 \times 10^{13}$ electrons per cm^2 results in a p–n junction with 800 meV electrostatic potential barrier. Unlike in a conventional p–n junction in graphene, in the case of the junction formed by an adsorbed organic molecular island we expect that the Klein tunneling is inhibited, even without an applied external magnetic field. Here Klein tunneling is inhibited by the ferromagnetic order that spontaneously occurs in the molecular island upon doping. We estimate that the magnetic barrier in the graphene sheet is around 10 mT.

PACS numbers: 73.22.-f, 71.15.Mb, 73.63.-b, 75.70.-i

Surface functionalization of graphene using organic molecules is a promising method to control doping of graphene. Among various organic molecules, tetrafluoro-tetracyanoquinodimethane (F_4TCNQ) is one of the most intensively studied organic dopants on graphene [1–7]. Since the electron affinity of F_4TCNQ is 5.24 eV[8] and the work function of graphene is 4.6 eV[9], the lowest unoccupied molecular orbital (LUMO) of the molecule lies well below the Dirac point of graphene and F_4TCNQ becomes an efficient p-type dopant when it is brought into contact with graphene. Most previous theoretical studies[10–13] of the F_4TCNQ /graphene system have been done considering a single molecule on a graphene sheet. However, recent experimental study found a self-assembled F_4TCNQ island[14] on a graphene substrate supported by insulating hexagonal boron nitride. This self-assembly is driven by the increase in the local work function as negatively charged molecules coalesce into an island [14].

With the formation of the island, the doping level can be controlled within a much wider range than for isolated molecules. For example, depositing naturally p-type molecular island onto an n-doped graphene would form a p–n junction in a graphene sheet; so that graphene sheet not covered in molecules remains n-type while graphene covered with molecules is p-type. This indicates that a 2D sheet of F_4TCNQ molecules could be a potential ingredient for fabricating useful graphene-based electronic devices.

A major obstacle for graphene-based electronics is the inability to confine Dirac electrons by electrostatic potentials, because of a unique characteristic of relativistic massless electrons known as Klein tunneling[15]. One way to inhibit the Klein tunneling is to open a band gap in graphene and consequently change the linear dispersive electronic property. However, this method strongly degrades the charge carrier mobility in the graphene layer

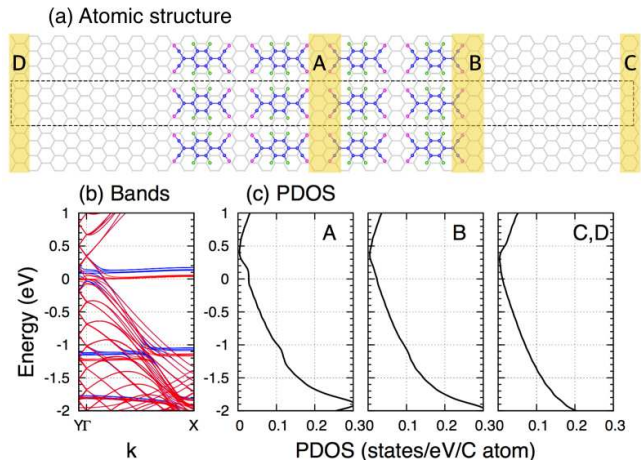


FIG. 1. (a) Atomic structure of an F_4TCNQ ribbon/graphene system. Graphene is shown with grey lines. Blue, pink, and green dots represent C, N, and F atoms constituting F_4TCNQ molecules, respectively. The dotted box shows the supercell used in our study. (b) Spin-resolved band structure with the Fermi level at zero energy and (c) projected density of states of the undoped case for region A, B, C, D shown in yellow. Majority and minority spins are indicated by red and blue colors, respectively.

which in turn hinders its application for electronic devices. Alternatively, inhomogeneous magnetic fields can be used to confine Dirac electrons without opening a band gap [16–20] and reducing the carrier mobility.

In this letter, we study the electrical and magnetic properties of a graphene sheet covered with a molecular F_4TCNQ ribbon [Fig. 1(a)]. We find that with electron doping the graphene sheet indeed forms a p–n junction. At the same time we find that the Klein tunneling through this p–n junction is reduced by the ferromagnetic moment formed on the F_4TCNQ molecules.

Our first-principles calculations are based on the use

of *ab-initio* norm-conserving pseudopotentials[21] and the Perdew-Burke-Ernzerhof-type[22] generalized gradient approximation to the density functional theory as implemented in the SIESTA code[23]. The electronic wavefunctions are expanded using pseudoatomic orbitals (double- ζ polarization). The charge density cutoff energy is 600 Ry and $32 \times 2 \times 1$ k -point sampling is used. To rule out the undesired interaction arising from the periodically arranged layers along the out-of-plane z direction, we placed ~ 100 Å vacuum gap between layers and included a dipole correction in all calculations.

Our periodic computational unit cell is shown with a dotted line in Fig. 1(a) and it contains a large graphene sheet with 288 carbon atoms. In order to simulate the finite size effect of the molecular island we cover half of the graphene sheet with densely packed F_4TCNQ molecules in the shape of a four-molecule wide ribbon with a width of 47 Å. The molecular ribbon (island) is periodically repeated along the perpendicular direction. The molecule is oriented in the ribbon so that its shorter axis is along the periodically repeated direction of the ribbon. Each F_4TCNQ molecule contains 20 atoms, so the total number of atoms in the computational unit cell is 368.

We first focus on the charge-neutral (undoped) case where the total ionic and electronic charge in the unit cell is zero. However, our calculation still allows for a charge transfer from the graphene sheet to the molecular island, as long as total charge remains zero. The calculated band structure for the undoped case is shown in Fig. 1(b). The nearly flat bands near the Fermi level and ~ 1 eV below the Fermi level originate from the molecular states, while the dispersive bands originate from the graphene sheet. We find that the graphene bands are spin-degenerate and the Dirac point is located 350 meV above the Fermi level since these organic molecules act as p-donors. To see the change of electronic properties in the graphene sheet depending on whether or not a ribbon is on it, we calculate the projected density of states (PDOS) for three areas: underneath the ribbon, the edge of the ribbon, and the area without a covered ribbon [Fig. 1(c)]. We find nearly no variation of the Dirac point in the three areas. Therefore all parts of graphene sheet in our periodic super-cell calculation are nearly equally p-doped by the molecular ribbon. We expect that with a wider super-cell, eventually graphene sheet would become neutral far away from the molecular ribbon.

The ground state of the neutral system is very weakly ferromagnetic. The energy difference between the ferromagnetic and nonmagnetic states is only 3 meV per one F_4TCNQ molecule. The flat band originating from the LUMO states of the F_4TCNQ molecule is split into one with the majority spin at the Fermi level and the other with the minority spin at 100 meV higher than the Fermi level [see Fig. 1(b)].

Now we focus on the electron-doped case. To explore the effect of doping, we added 2 extra electrons in our

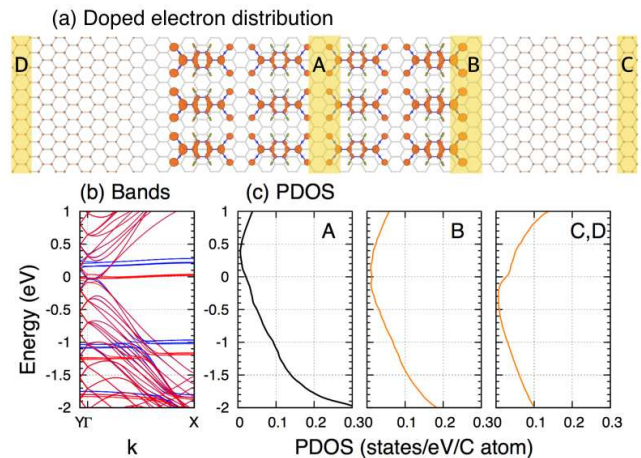


FIG. 2. (a) The spatial distribution of doped electrons when the system is doped with two electrons per cell. The isosurface with electron density of 2.7 nm^{-3} is shown with an orange surface. (b) Spin-resolved band structure and (c) projected density of states of the electron-doped case for region A, B, C, D are shown in yellow. Majority and minority spins are indicated by red and blue colors, respectively.

computational unit cell that contains 4 molecules. We estimated the average electron density to be 2.7×10^{13} electrons/cm² by dividing the added charge by the area of the computational unit cell. Such a doping level can be achieved via employing an electrolyte gate [24–27]. After relaxation of the added charge we find that graphene underneath the island remains unaffected. Namely, graphene underneath the molecular island remains p-doped even with excess electrons in the unit cell [see Fig. 2(a)]. Instead, excess electron charge accumulates in the molecular island and in the graphene that is not covered with molecules. We find that about 40 % of the inserted electron charge accumulate on the ribbon while the remaining 60 % of the charge goes into the uncovered part of the graphene.

The excess charge in the uncovered graphene causes its Dirac point to sink below the Fermi level and it therefore becomes n-type doped. Since the graphene underneath the ribbon remained p-type we conclude that the electron doping of the F_4TCNQ island on graphene forms a p–n junction in the graphene sheet. This charge configuration is consistent with the fact that the positively charged molecular island repels electrons from the graphene underneath the island.

The projected density of states analysis reveals that in the uncovered graphene the energy difference between the Dirac point and the Fermi level shifts by 800 meV [Fig. 2(c)] relative to the neutral case.

Although this molecular island forms an effective electrostatic potential barrier, this is not sufficient to confine the Dirac electrons because of the Klein tunneling effect mentioned earlier. Nevertheless, the Klein tunnel-

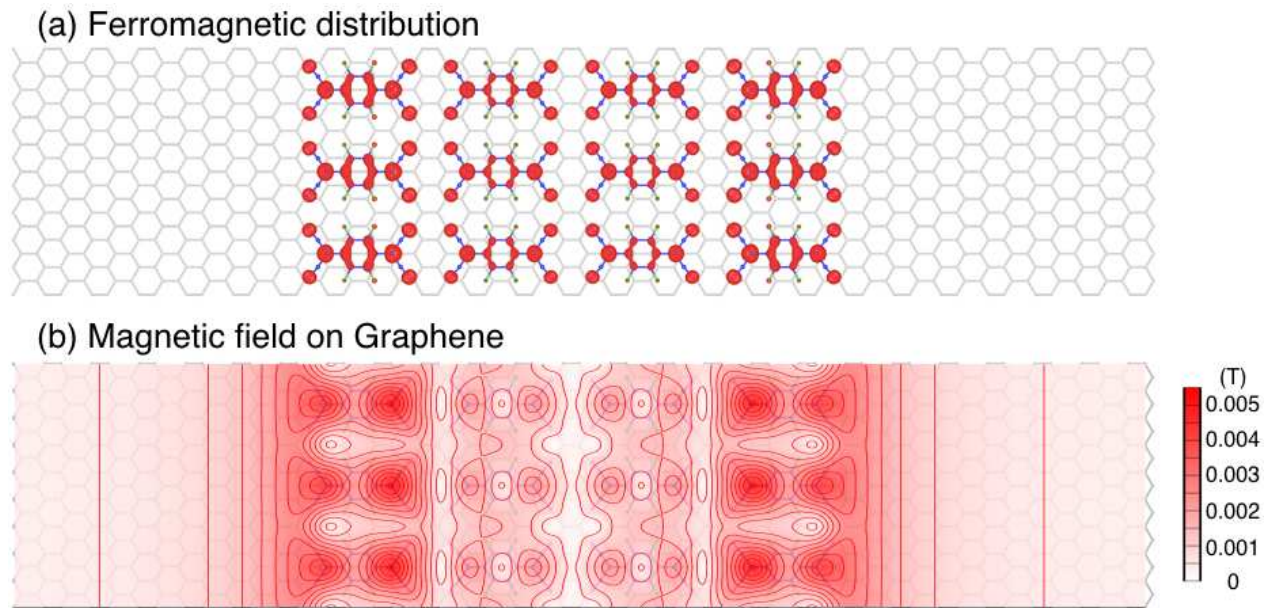


FIG. 3. (a) Charge density difference between the majority spin and minority spin configurations. The isosurface with electron density of 6.7 nm^{-3} is shown in red. (b) The magnitude of the magnetic field on graphene. Isolines are drawn at intervals of 0.5 mT. Both figures are for the case when the system is doped with two electrons per cell.

ing is inhibited in the F₄TCNQ ribbon/graphene system because electron doping changes not only the electronic properties but also the magnetic properties of the system.

In addition to the formation of the p-n junction, electron doping enhances the stability of ferromagnetic state and increases the ferromagnetic moment in F₄TCNQ ribbon. When 2 electrons are added in the computational unit cell (corresponding to 2.7×10^{13} electrons/cm²), the energy difference between the ferromagnetic and non-magnetic states is increased from 3 meV/molecule to 21 meV/molecule. The net ferromagnetic moment is calculated to be $0.85 \mu_B/4$ molecules for the undoped case and $1.81 \mu_B/4$ molecules for the 2-electron-doped case.

The physical origin of the enhanced magnetism upon electron doping for this system can be attributed to the Coulomb interaction within the molecule. Since the states of the F₄TCNQ molecules are spatially localized within each molecule [Fig. 3(a)], the electrons in the ribbon can be described using a Hubbard model. In the Hubbard model, the energy gain due to spin polarization is proportional to the square of the total number of electrons [28]. According to the theory, when the total number of electrons in the ribbon increases from 0.85 to 1.81, the energy gain with full polarization is enhanced a factor of 4.5, which is comparable to the calculated result.

To make a quantitative prediction of how the Klein tunneling can be inhibited by the magnetism of F₄TCNQ ribbon, we calculate the magnetic field on a graphene sheet when the net ferromagnetic moment in the super-cell is $1.81 \mu_B$. For the calculation, the following equation

is used,

$$\mathbf{B}(\mathbf{r}) = \nabla \times \frac{\mu_0}{4\pi} \iiint_{all} \frac{\mathbf{m}(\mathbf{r}') \times (\mathbf{r} - \mathbf{r}')}{|\mathbf{r} - \mathbf{r}'|^3} dV' \quad (1)$$

where $|\iiint_{cell} \mathbf{m}(\mathbf{r}') dV'| = 1.81 \mu_B$ and $\mathbf{m}(\mathbf{r})$ is proportional to the difference between the majority and minority spin-polarized charge density computed from first-principles. The resulting calculated magnetic field $|\mathbf{B}(\mathbf{r})|$ in the graphene sheet is drawn using a color plot in Fig. 3(b). The maximum value (~ 5 mT) appears under the edge of the ribbon. The field below the inner molecules is reduced to 2.2 mT and it becomes less than 0.5 mT away from the ribbon. We expect that with a wider super-cell, the magnetic field away from the ribbon would eventually go to zero. The difference in the magnetic field between the edge and the interior of the ribbon is caused by the variation of the magnetic moment along the ribbon. For example, magnetic moment on the molecule at the ribbon edge is 1.4 times larger than in the interior.

If the system is doped with even more electrons (approximately 5.3×10^{13} electrons/cm²), the net ferromagnetic moment can be increased up to $4 \mu_B$. With this maximum moment, Dirac electrons passing under the F₄TCNQ ribbon will encounter a ~ 10 mT magnetic field barrier. If the height of the magnetic barrier is assumed to be constant within the ribbon, the magnetic length $l_B = \sqrt{\hbar/eB}$ becomes 250 nm. When the energy of incoming state, ε , satisfies the following condition

$$\varepsilon \frac{l_B}{\hbar v_f} \leq \frac{d}{l_B} \quad (2)$$

where v_f is the Fermi velocity ($\simeq 1 \times 10^6$ m/s) and $2d$ is the width of a ribbon, the incoming state is reflected regardless of the incidence angle [16]. So, if the width of the F_4TCNQ ribbon is extended to 500 nm, then every incoming state with energy less than 2.5 meV is totally reflected at the boundary with p-n junction configuration.

Moreover, an unique inhomogeneous magnetic and electrostatic barrier geometry in one dimension could be realized by applying homogeneous perpendicular weak magnetic field on the entire system. The directions of the magnetic field inside and outside F_4TCNQ ribbon can either be parallel or anti-parallel. From previous theoretical studies[18, 29–31], robust one-dimensional conducting edge states are predicted for such a barrier geometry. Those edge states have a possibility to be realized in F_4TCNQ ribbon/graphene system, and this system may show a very large magnetoresistance behavior.

In conclusion, we studied the electric and magnetic properties of an F_4TCNQ ribbon/graphene system. We find that, when the system is doped with extra electrons, only the uncovered part of the graphene is doped. This lowers the Dirac point energy below the Fermi level making a p-n junction configuration in the graphene sheet. Furthermore, we find that electron doping induces tunable ferromagnetism in the ribbon. When extra electrons flow into the system, the ferromagnetic moment in the ribbon is increased and that moment produces the magnetic barrier high enough to confine Dirac electrons. Our findings reveal the possibility of tunable electrostatic and magnetic barriers in graphene, which could be effective for inhibiting Klein tunneling in graphene-based electronic devices.

This work was supported by National Science Foundation Grant No. DMR15-1508412 (electronic structure calculation) and by the Director, Office of Science, Office of Basic Energy Sciences, Materials Sciences and Engineering Division, U.S. Department of Energy under Contract No. DE-AC02-05CH11231, within the SP2 Program (magnetic structure calculation). Y.-W. S. was supported in part by the NRF funded by the MSIP of the Korean government (CASE, No. 2011-0031640). Computational resources have been provided by the DOE at Lawrence Berkeley National Laboratory's NERSC facility.

* Email: xtom97@hanmail.net

- [1] K. S. Mali, J. Greenwood, J. Adisojoso, R. Phillipson, and S. D. Feyter, *Nanoscale* **7**, 1566 (2015).
- [2] J. M. MacLeod and F. Rosei, *Small* **10**, 1038 (2014).
- [3] G. Hong, Q.-H. Wu, J. Ren, C. Wang, W. Zhang, and S.-T. Lee, *Nano Today* **8**, 388 (2013).
- [4] W. Chen, S. Chen, D. C. Qi, X. Y. Gao, and A. T. S. Wee, *J. Am. Chem. Soc.* **129**, 10418 (2007).
- [5] J. Song, F.-Y. Kam, R.-Q. Png, W.-L. Seah, J.-M. Zhuo, G.-K. Lim, P. K. H. Ho, and L.-L. Chua, *Nat. Nanotechnol.* **8**, 356 (2013).
- [6] X. Wang, J.-B. Xu, W. Xie, and J. Du, *J. Phys. Chem. C* **115**, 7596 (2011).
- [7] D. Maccariello, M. Garnica, M. A. Niño, C. Navío, P. Perna, S. Barja, A. L. Vázquez de Parga, and R. Miranda, *Chem. Mater.* **26**, 2883 (2014).
- [8] C. Coletti, C. Riedl, D. S. Lee, B. Krauss, L. Patthey, K. von Klitzing, J. H. Smet, and U. Starke, *Phys. Rev. B* **81**, 235401 (2010).
- [9] Y.-J. Yu, Y. Zhao, S. Ryu, L. E. Brus, K. S. Kim, and P. Kim, *Nano Lett.* **9**, 3430 (2009).
- [10] H. Pinto, R. Jones, J. P. Goss, and P. R. Briddon, *J. Phys.: Condens. Matter* **21**, 402001 (2009).
- [11] J. T. Sun, Y. H. Lu, W. Chen, Y. P. Feng, and A. T. S. Wee, *Phys. Rev. B* **81**, 155403 (2010).
- [12] M. Garnica, D. Stradi, S. Barja, F. Calleja, C. Díaz, M. Alcamí, N. Martín, A. L. Vázquez de Parga, F. Martín, and R. Miranda, *Nat. Phys.* **9**, 368 (2013).
- [13] D. Stradi, M. Garnica, C. Díaz, F. Calleja, S. Barja, N. Martín, M. Alcamí, A. L. Vázquez de Parga, R. Miranda, and F. Martín, *Nanoscale* **6**, 15271 (2014).
- [14] H.-Z. Tsai, A. A. Omrani, S. Coh, H. Oh, S. Wickenburg, Y.-W. Son, D. Wong, A. Riss, H. S. Jung, G. D. Nguyen, G. F. Rodgers, A. S. Aikawa, T. Taniguchi, K. Watanabe, A. Zettl, S. G. Louie, J. Lu, M. L. Cohen, and M. F. Crommie, *ACS Nano* **9**, 12168 (2015).
- [15] M. I. Katsnelson, K. S. Novoselov, and A. K. Geim, *Nat. Phys.* **2**, 620 (2006).
- [16] A. De Martino, L. Dell'Anna, and R. Egger, *Phys. Rev. Lett.* **98**, 066802 (2007).
- [17] A. V. Shytov, M. S. Rudner, and L. S. Levitov, *Phys. Rev. Lett.* **101**, 156804 (2008).
- [18] A. V. Rozhkov, G. Giavaras, Y. P. Bliokh, V. Freilikher, and F. Nori, *Physics Reports* **503**, 77 (2011).
- [19] A. F. Young and P. Kim, *Annual Review of Condensed Matter Physics* **2**, 101 (2011).
- [20] W.-T. Lu, C.-T. Xu, C.-Z. Ye, H. Jiang, H.-Z. Pan, and Y.-L. Wang, *Phys. Lett. A* **379**, 1906 (2015).
- [21] D. R. Hamann, M. Schlüter, and C. Chiang, *Phys. Rev. Lett.* **43**, 1494 (1979).
- [22] J. P. Perdew, K. Burke, and M. Ernzerhof, *Phys. Rev. Lett.* **77**, 3865 (1996).
- [23] D. Sánchez-Portal, P. Ordejón, E. Artacho, and J. M. Soler, *Int. J. Quantum Chem.* **65**, 453 (1997).
- [24] A. Das, S. Pisana, B. Chakraborty, S. Piscanec, S. K. Saha, U. V. Waghmare, K. S. Novoselov, H. R. Krishnamurthy, A. K. Geim, A. C. Ferrari, and A. K. Sood, *Nat. Nanotechnol.* **3**, 210 (2008).
- [25] K. F. Mak, C. H. Lui, J. Shan, and T. F. Heinz, *Phys. Rev. Lett.* **102**, 256405 (2009).
- [26] D. K. Efetov and P. Kim, *Phys. Rev. Lett.* **105**, 256805 (2010).
- [27] J. Ye, M. F. Craciun, M. Koshino, S. Russo, S. Inoue, H. Yuan, H. Shimotani, A. F. Morpurgo, and Y. Iwasa, *Proc. Natl. Acad. Sci. USA* **108**, 13002 (2011).
- [28] J. Hubbard, *Proc. Roy. Soc. London A* **276**, 238 (1963).
- [29] S. Park and H.-S. Sim, *Phys. Rev. B* **77**, 075433 (2008).
- [30] T. K. Ghosh, A. De Martino, W. Häusler, L. Dell'Anna, and R. Egger, *Phys. Rev. B* **77**, 081404(R) (2008).
- [31] L. Oroszlány, P. Rakyta, A. Kormányos, C. J. Lambert, and J. Cserti, *Phys. Rev. B* **77**, 081403(R) (2008).